Progress In Electromagnetics Research, Vol. 146, 47–56, 2014

Near-Field Time-Domain Shielding Effectiveness of Thin Conductive Screens

Giampiero Lovat*, Rodolfo Araneo, and Salvatore Celozzi

Abstract—The time-domain shielding effectiveness of planar conductive thin screens excited by a transient electric-line source is studied in detail by means of an approximate semi-analytical formulation based on a Cagniard-De Hoop approach. Such a formulation allows for easily deriving and discussing several definitions of time-domain shielding effectiveness, recently introduced in the literature. Comparisons with results obtained numerically through an exact canonical double inverse Fourier transform are provided which furnish a benchmark to discuss the advantages and limits of the proposed approximate formulation.

1. INTRODUCTION

The transient analysis of electromagnetic fields due to non-harmonic sources is an issue which is recently regaining interest and importance because of the current research focused on ultrawideband systems and high-clock-rate digital processors. On the other hand, several transient phenomena may require the evaluation of a shielding performance [1]: the classical shielding effectiveness (SE) evaluated in the frequency domain may be unsuitable for a direct interpretation and use in transient shielding problems because of two reasons: *i)* usually, only the amplitude spectra of the external source are accounted for and nothing is said about the phases of the harmonics which may actually sum or subtract in the time-domain waveform and *ii)* no direct information about the protection level achievable by means of any configuration is provided: only the reduction of each harmonic, but nothing can be argued about, e.g., induced effects due to time derivative of the magnetic flux. For these reasons, new figures of merit have recently been proposed for the evaluation of the SE of shielding structures under a transient excitation [2, 3]. Such new parameters obviously require the accurate knowledge of the transient field generated by the source of the electromagnetic field.

The most classical shielding problem consists in the evaluation of the performance of an infinite planar screen [4]. In the literature, several types of planar screens have been considered (including metamaterial and periodic screens), under *time-harmonic* plane-wave, line, and dipole excitations [5–7]. However, when a transient source is considered, the solution is not trivial [8, 9], and must be derived numerically even in simple geometries through a double integral which corresponds to two synthesis steps: first, the frequency-domain (FD) solution is obtained via a spatial-wavenumber synthesis (usually expressed as a Sommerfeld integral) and then the time-domain (TD) solution via a frequency synthesis (by performing another integration over the frequency range). Usually these integrals are highly oscillatory and slow-decaying thus making the process very time-consuming.

On the other hand, the Cagniard-De Hoop technique is recognized to be a powerful method for analyzing the transient fields radiated by a finite source in a general multilayered environment [10, 11] and recently the method has been applied to the evaluation of the field generated by a pulsed electric line source in the presence of a thin sheet with high contrasts in its conductive and dielectric properties

Received 10 March 2014, Accepted 8 April 2014, Scheduled 18 April 2014

* Corresponding author: Giampiero Lovat (giampiero.lovat@uniroma1.it).

The authors are with the Electrical Engineering Division of DIAEE, University of Rome "La Sapienza", Via Eudossiana 18, Roma 00184, Italy.

with respect to the embedding free space [12], leading to numerically simple results for the relevant fields.

By following [12], in this work we derive a simple closed-form expression for the potential TD Green's function of a thin conductive screen in the presence of an electric line source. The approximation consists in representing the conductive screen through a sheet conductance and by assuming that such a representation remains valid over the entire frequency range which is responsible of the frequency synthesis. This allows obtaining the field emitted by a transient electric line source by means of a simple time-convolution. By using this result, several definitions of time-domain shielding effectiveness (TD SE) recently introduced in the literature can be discussed in detail. The limits of accuracy of the proposed semi-analytical formulation are finally discussed through a comparison with results obtained by means of a numerical procedure based on the exact expressions.

2. NUMERICAL SYNTHESIS OF FIELD SOLUTION

The problem under analysis is sketched in Fig. 1. A pulsed electric line source $\mathbf{J}_i(\mathbf{r},t) = i(t)\delta(x - x_0)\delta(z - z_0)\mathbf{u}_y$ placed in the half-space $z > 0$ radiates in the presence of a planar conductive slab of thickness h and conductivity σ: we are interested in evaluating the relevant TE field (h_x, e_y, h_z) in the halfspace $z < 0$. The two-dimensional (2-D) spectral-domain (SD) potential Green's function $\tilde{G}_A(k_x, \omega; z, z_0)$ of the problem can be derived as [13]

$$\tilde{G}_A(k_x, \omega; \Delta z) = \left(\frac{1}{j\omega}\right) \frac{Y_{\mathrm{s}} e^{-jk_{z0}(\Delta z - h)}}{2Y_0 Y_{\mathrm{s}} \cos(k_{z\mathrm{s}} h) + j\left(Y_0^2 + Y_{\mathrm{s}}^2\right) \sin(k_{z\mathrm{s}} h)} \tag{1}$$

where

$$k_{z0}^2 = (\omega/c_0)^2 - k_x^2, \quad k_{z\mathrm{s}}^2 = k_{z0}^2 - j\omega\mu_0\sigma,$$

$Y_0 = k_{z0}/(\omega\mu_0)$, $Y_{\mathrm{s}} = k_{z\mathrm{s}}/(\omega\mu_0)$, $\Delta z = z_0 - z$, and c_0 is the speed of light in free space. Expression (1) can then be used to derive the SD electric field $\tilde{E}_y$ as [13]

$$\tilde{E}_y(k_x, \omega; \Delta z) = -j\omega \tilde{G}_A(k_x, \omega; \Delta z)\, I(\omega) \tag{2}$$

where $I(\omega)$ is the Fourier transform of $i(t)$. Thus the TD electric field is obtained through a double inverse Fourier transform as

$$e_y(\mathbf{r}, t) = \frac{1}{2\pi} \int_{-\infty - ja}^{+\infty - ja} E_y(\mathbf{r}, \omega)\, e^{j\omega t}\, \mathrm{d}\omega \tag{3}$$

where $a > 0$ and

$$E_y(\mathbf{r}, \omega) = \frac{1}{2\pi} \int_{-\infty}^{+\infty} \tilde{E}_y(k_x, \omega; z, z_0)\, e^{-jk_x \Delta x}\, \mathrm{d}k_x. \tag{4}$$

The components of the transient magnetic field $h_x(\mathbf{r}, t)$ and $h_z(\mathbf{r}, t)$ can also be derived with a similar procedure, starting from the relevant SD expressions [13]:

$$\tilde{H}_x(k_x, \omega; \Delta z) = j\frac{k_{z0}}{\mu_0}\, \tilde{G}_A(k_x, \omega; \Delta z)\, I(\omega) \tag{5}$$

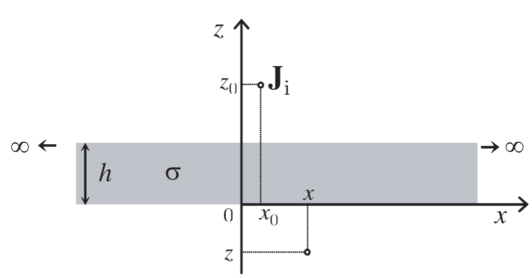

Figure 1. Transient electric line source in the presence of a thin conductive screen.

and

$$\tilde{H}_z\left(k_x,\omega;\Delta z\right) = -j\frac{k_x}{\mu_0}\tilde{G}_A\left(k_x,\omega;\Delta z\right)I\left(\omega\right). \tag{6}$$

To accelerate the calculation of the possibly oscillatory integrals (3) and (4), several methods can be applied [14].

3. SEMI-ANALYTICAL SOLUTION

For thin slabs, the screen can be approximately modeled through a sheet-boundary condition, i.e., in a transverse-equivalent-network representation [13] as a shunt conductance $G_\sigma = \sigma h$. An approximate expression for $\tilde{G}_A$ is then achieved as

$$\tilde{G}_A\left(k_x,\omega;\Delta z\right) \simeq -j\mu_0\frac{e^{-jk_{z0}\Delta z}}{2k_{z0}+\omega\mu_0 G_\sigma}. \tag{7}$$

The FD representation of the potential Green's function is

$$G_A\left(\mathbf{r},\omega\right) = \frac{1}{2\pi}\int_{-\infty}^{+\infty}\tilde{G}_A\left(k_x,\omega;\Delta z\right)e^{-jk_x\Delta x}\,\mathrm{d}k_x. \tag{8}$$

By adopting the wave slowness-domain representation [15] with the change of variables $s = j\omega$ and $p = jk_x/s$, from (8) and (7) we have

$$G_A\left(\mathbf{r},s\right) = \frac{\mu_0}{2\pi j}\int_{-j\infty+a}^{+j\infty+a}\frac{e^{-s[p\Delta x+\gamma(p)\Delta z]}}{2\gamma\left(p\right)+\mu_0 G_\sigma}\,\mathrm{d}p \tag{9}$$

where

$$\gamma\left(p\right) = \sqrt{\frac{1}{c_0^2}-p^2}. \tag{10}$$

By using a classical modified Cagniard-De Hoop method [16], the two-dimensional TD potential Green's function can be obtained in a simple closed form. In fact, by deforming the integration path $\Re\mathrm{e}\{p\} = a$ in the complex p plane until the integral resemble a Laplace transformation with a real (time) parameter, by means of the Cauchy theorem and the Jordan lemma [15], we can replace the original contour with the Cagniard-De Hoop path defined by

$$\tau = p\Delta x + \gamma\left(p\right)\Delta z. \tag{11}$$

Solving (11) for p we obtain the hyperbolic contour parametrization

$$p\left(\tau\right) = \frac{\tau\Delta x \pm j\sqrt{\tau^2-T_0^2}\,dz}{D^2} \tag{12}$$

where $D = \left(\Delta x^2+\Delta z^2\right)^{1/2}$ indicates the source-observation point distance and $T_0 = D/c_0$ the least-travel time for a disturbance from the source to reach the observer. By using the Schwartz reflection principle to combine the contributions from the upper and lower hyperbolic arcs we have

$$G_A\left(\mathbf{r},s\right) = \frac{\mu_0}{2\pi}\int_0^{+\infty}\Re\mathrm{e}\left\{\frac{2\gamma\left(\hat{p}\right)}{2\gamma\left(\hat{p}\right)+\mu_0 G_\sigma}\right\}e^{-s\tau}\frac{H\left(t-\tau\right)}{\sqrt{t^2-T_0^2}}\,\mathrm{d}\tau \tag{13}$$

where $H\left(\cdot\right)$ stands for the Heaviside unit-step function and $\hat{p}$ indicates the upper arc (plus sign) in (12) so that

$$\gamma\left(\hat{p}\right) = \frac{\tau\Delta z - j\sqrt{\tau^2-T_0^2}\,dx}{D^2}. \tag{14}$$

From (13) we thus easily obtain

$$g_A\left(\mathbf{r},t\right) = \frac{\mu_0}{2\pi}\Re\mathrm{e}\left\{\frac{2\gamma\left(\hat{p}\right)}{2\gamma\left(\hat{p}\right)+\mu_0 G_\sigma}\right\}\frac{H\left(t-\tau\right)}{\sqrt{t^2-T_0^2}} = \frac{\mu_0}{2\pi}\frac{t^2+\alpha\Delta zt-T_x^2}{t^2+2\alpha\Delta zt+\alpha^2D^2-T_x^2}\frac{H(t-T_0)}{\sqrt{t^2-T_0^2}} \tag{15}$$

where $\alpha = \mu_0 G_\sigma/2$ and $T_x = \Delta x/c_0$. Expression (15) is consistent with the 2-D TD potential Green's function in free space ($\sigma = 0$, i.e., $\alpha = 0$) [11]

$$g_A^{\mathrm{FS}}(\mathbf{r},t) = \frac{\mu_0}{2\pi}\frac{H(t-T_0)}{\sqrt{t^2-T_0^2}}\,. \tag{16}$$

From (2), the space-time representation of the electric field can be obtained as

$$e_y(\mathbf{r},t) = -\frac{\partial}{\partial t}\int_{-\infty}^{+\infty} g_A(\mathbf{r},\tau)\, i(t-\tau)\,\mathrm{d}\tau = -\int_{-\infty}^{+\infty} g_A(\mathbf{r},\tau)\left.\frac{\mathrm{d}i}{\mathrm{d}t}\right|_{t-\tau}\mathrm{d}\tau \tag{17}$$

By assuming, with a little abuse of notation, that $i(t) = i(t)\,H(t)$ and $g_A(\mathbf{r},t) = g_A(\mathbf{r},t)\,H(t-T_0)$, we can also express

$$e_y(\mathbf{r},t) = -\int_{T_0}^{t} g_A(\mathbf{r},\tau)\left.\frac{\mathrm{d}i}{\mathrm{d}t}\right|_{t-\tau}\mathrm{d}\tau \tag{18}$$

provided that $i(0) = 0$. Because of the inverse square-root singularity in the $g_A(\mathbf{r},\tau)$ function, a simple change of variable can be performed in (18) in order to make easier the numerical evaluation of the time-convolution integral.

To obtain the transient magnetic field one can still follow a similar Cagniard-De Hoop procedure thus obtaining

$$h_i(\mathbf{r},t) = \frac{\partial}{\partial t}\int_{-\infty}^{+\infty} g_i(\mathbf{r},\tau)\, i(t-\tau)\,\mathrm{d}\tau\,, \qquad i = x, z \tag{19}$$

where

$$g_x(\mathbf{r},t) = \frac{1}{2\pi}\,\Re\mathrm{e}\left\{\frac{2\gamma^2(\hat{p})}{2\gamma(\hat{p})+\mu_0 G_\sigma}\right\}\frac{H(t-\tau)}{\sqrt{t^2-T_0^2}} = \frac{1}{2\pi D^2}\,\frac{\Delta z t^3 + \alpha D^2 t^2 - \Delta z T_x^2 t + \alpha D^2 T_x^2}{t^2 + 2\alpha\Delta z t + \alpha^2 D^2 - T_x^2}\,\frac{H(t-T_0)}{\sqrt{t^2-T_0^2}} \tag{20}$$

and

$$g_z(\mathbf{r},t) = -\frac{1}{2\pi}\,\Re\mathrm{e}\left\{\frac{2\hat{p}\gamma(\hat{p})}{2\gamma(\hat{p})+\mu_0 G_\sigma}\right\}\frac{H(t-\tau)}{\sqrt{t^2-T_0^2}} = -\frac{\Delta x}{2\pi D^2}\,\frac{t^3 + 2\alpha\Delta z t^2 - T_x^2 t - \alpha D^2\Delta z/c_0^2}{t^2 + 2\alpha\Delta z t + \alpha^2 D^2 - T_x^2}\,\frac{H(t-T_0)}{\sqrt{t^2-T_0^2}} \tag{21}$$

so that eventually we have

$$h_i(\mathbf{r},t) = \int_{T_0}^{t} g_i(\mathbf{r},\tau)\left.\frac{\mathrm{d}i}{\mathrm{d}t}\right|_{t-\tau}\mathrm{d}\tau\,, \qquad i = x, z. \tag{22}$$

As it will be shown in Section 5, the TD SE definitions require the calculation of the time derivative of the field components. It is thus simple to show that

$$\frac{\partial e_y}{\partial t} = -\int_{T_0}^{t} g_A(\mathbf{r},\tau)\left.\frac{\mathrm{d}^2 i}{\mathrm{d}t^2}\right|_{t-\tau}\mathrm{d}\tau \tag{23}$$

and

$$\frac{\partial h_i}{\partial t} = \int_{T_0}^{t} g_i(\mathbf{r},\tau)\left.\frac{\mathrm{d}^2 i}{\mathrm{d}t^2}\right|_{t-\tau}\mathrm{d}\tau\,, \qquad i = x, z. \tag{24}$$

provided that $i(0) = \left.\mathrm{d}i/\mathrm{d}t\right|_{t=0} = 0$.

4. CLASSICAL TRANSIENT SOURCES

Two types of transient electric-line sources are introduced and used in the numerical results, i.e., the power exponential pulse (PEP) and the monocycle pulse (MP) which represent electric currents associated with the discharge of a capacitor in a resistive circuit and an electric current flowing in a closed conducting loop, respectively [12]. The relevant expressions are

$$i_{\mathrm{PEP}}(t) = I_0\left(\frac{t}{T_\mathrm{c}}\right)^n \exp\left[-n\left(\frac{t}{T_\mathrm{c}}-1\right)\right] H(t) \tag{25}$$

and

$$i_{\mathrm{MP}}(t) = I_0 N(n) \left(1 - \frac{t}{T_\mathrm{c}}\right) \left(\frac{t}{T_\mathrm{c}}\right)^{n-1} \exp\left[-n\left(\frac{t}{T_\mathrm{c}} - 1\right)\right] H(t) \tag{26}$$

where

$$N(n) = \sqrt{n} \left(\frac{1}{1 - \frac{1}{\sqrt{n}}}\right)^{n-1} e^{-\sqrt{n}} \tag{27}$$

is a normalization factor and $n > 2$ in order to have C^2 functions (so that $i(0) = \left.\mathrm{d}i/\mathrm{d}t\right|_{t=0} = 0$). The relevant FD Fourier transforms are

$$I_{\mathrm{PEP}}(\omega) = I_0 T_\mathrm{c} \left(\frac{e}{n}\right)^n \frac{\Gamma(n)}{\left[1 + q^2(\omega)\right]^{\frac{n+1}{2}}} e^{-j(n+1)\phi(\omega)} \tag{28}$$

and

$$I_{\mathrm{MP}}(\omega) = I_0 T_\mathrm{c} N(n) \frac{jq(\omega)}{1 + jq(\omega)} \left(\frac{e}{n}\right)^n \frac{\Gamma(n)}{\left[1 + q^2(\omega)\right]^{\frac{n}{2}}} e^{-jn\phi(\omega)} \tag{29}$$

where $\Gamma(\cdot)$ is the Euler gamma function, $q(\omega) = \omega T_\mathrm{c}/n$, and $\phi(\omega) = \arctan q(\omega)$.

5. TIME-DOMAIN SHIELDING EFFECTIVENESS

The issue of the suitable definition of SE has recently been addressed [2, 17]. In particular, in the TD two local parameters have been introduced, i.e.,

$$\begin{aligned}
\mathrm{SE}_{\mathrm{PR}}^{\mathrm{E}}(\mathbf{r}) &= 20 \log \frac{\max_t \left|\mathbf{e}^{\mathrm{inc}}(\mathbf{r}, t)\right|}{\max_t \left|\mathbf{e}(\mathbf{r}, t)\right|} \\
\mathrm{SE}_{\mathrm{PR}}^{\mathrm{H}}(\mathbf{r}) &= 20 \log \frac{\max_t \left|\mathbf{h}^{\mathrm{inc}}(\mathbf{r}, t)\right|}{\max_t \left|\mathbf{h}(\mathbf{r}, t)\right|}
\end{aligned} \tag{30}$$

where $\mathbf{e}^{\mathrm{inc}}(\cdot)$ and $\mathbf{h}^{\mathrm{inc}}(\cdot)$ indicate the incident electric and magnetic field, respectively, i.e., the electric and magnetic fields at the observation point in the absence of the screen. It should be noted that the $\mathrm{SE}_{\mathrm{PR}}$ parameters are based on the peak-value reduction of the electric- or magnetic-field waveforms.

The second set of parameters account for the limitation of the induced effects associated with the time-derivative of the magnetic and electric fields, i.e.,

$$\begin{aligned}
\mathrm{SE}_{\mathrm{DR}}^{\mathrm{E}}(\mathbf{r}) &= 20 \log \frac{\max_t \left|\frac{\partial \mathbf{e}^{\mathrm{inc}}}{\partial t}\right|}{\max_t \left|\frac{\partial \mathbf{e}}{\partial t}\right|} \\
\mathrm{SE}_{\mathrm{DR}}^{\mathrm{H}}(\mathbf{r}) &= 20 \log \frac{\max_t \left|\frac{\partial \mathbf{h}^{\mathrm{inc}}}{\partial t}\right|}{\max_t \left|\frac{\partial \mathbf{h}}{\partial t}\right|}
\end{aligned} \tag{31}$$

In TD-SE evaluations for infinite planar screens it is usually assumed that $x = x_0$ (i.e., $\Delta x = 0$) and the expressions in (15), (20), and (21) take the simpler form

$$\begin{aligned}
g_A(\mathbf{r}, t) &= \frac{\mu_0}{2\pi} \frac{t}{(t + \alpha\Delta z)\sqrt{t^2 - T_0^2}} H(t - T_0) \\
g_x(\mathbf{r}, t) &= \frac{1}{2\pi\Delta z} \frac{t^2}{(t + \alpha\Delta z)\sqrt{t^2 - T_0^2}} H(t - T_0) \\
g_z(\mathbf{r}, t) &= 0
\end{aligned} \tag{32}$$

with $T_0 = \Delta z / c_0$.

6. LIMITS OF VALIDITY OF THE SEMI-ANALYTICAL FORMULATION

The proposed semi-analytical formulation which allows to calculate the EM field due to a transient line source by means of a simple time convolution is numerically very convenient and accurate provided that the basic assumption is satisfied, i.e., (7) is an accurate approximation of (1). For conductive media, this means that we can expand the trigonometric functions in (1) to the first order, i.e.,

$$h\sqrt{\omega\mu_0\sigma} \ll 1 \tag{33}$$

Obviously, (33) must remain valid for all the frequencies which give a significant contribution in the frequency synthesis of the EM field. The maximum frequency $\omega_{\max}$ for which (33) is required to hold strongly depends on the source characteristics. For instance, if we consider the PEP source and define $\omega_{\max}$ as that frequency for which the amplitude of the source has decayed by a 10^d factor with respect to its maximum, it is simple to show that it results

$$\omega_{\max} = \frac{n}{T_c}\sqrt{10^{\frac{2d}{n+1}} - 1} \tag{34}$$

so that we assume that (7) is an accurate approximation of (1) provided that

$$h^2\omega_{\max}^2\mu_0\sigma < 10^{-2}. \tag{35}$$

Equation (35) provides a constraint for the metal conductivity σ, the screen thickness h, and the characteristic time of the source T_c, i.e.,

$$T_c > 100n\sqrt{10^{\frac{2d}{n+1}} - 1}\,\mu_0\sigma h^2 \tag{36}$$

As an example, by considering a copper screen with $\sigma = 5.8 \cdot 10^7$ S/m and $h = 30\,\mu$m (and $n = 16$ and $d = 3$ as additional parameters), it results $T_c > 120\,\mu$s. To confirm the above analysis, in Fig. 2(a) the FD electric field calculated through the exact (1) and approximate (7) SD Green's function is reported as a function of ω for $T_c = 200\,\mu$s and $T_c = 10$ ns (with $\Delta x = 0$ and $\Delta z = 20$ cm). Moreover, in Fig. 2(b) the relevant TD electric fields (exact and approximate) are reported as functions of t/T_c. It can thus be seen that the apparently small error in the FD (as in the case of $T_c = 10$ ns) can lead to completely erroneous results in the TD. On the other hand the TD fields when $T_c = 200\,\mu$s are completely superimposed.

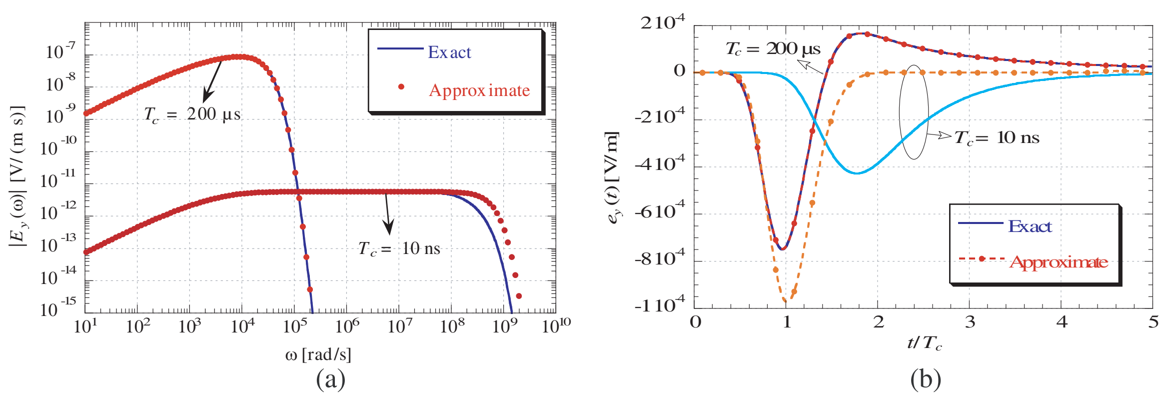

Figure 2. Electric fields calculated through the exact and approximate SD Green's functions as functions of ω for $T_c = 200\,\mu$s and $T_c = 10$ ns: (a) FD as functions of the radian frequency ω and (b) TD as functions of t/T_c. Parameters: $\sigma = 5.8 \cdot 10^7$ S, $h = 30\,\mu$m, $\Delta x = 0$, $\Delta z = 20$ cm, PEP source with $I_0 = 1$ A and $n = 16$.

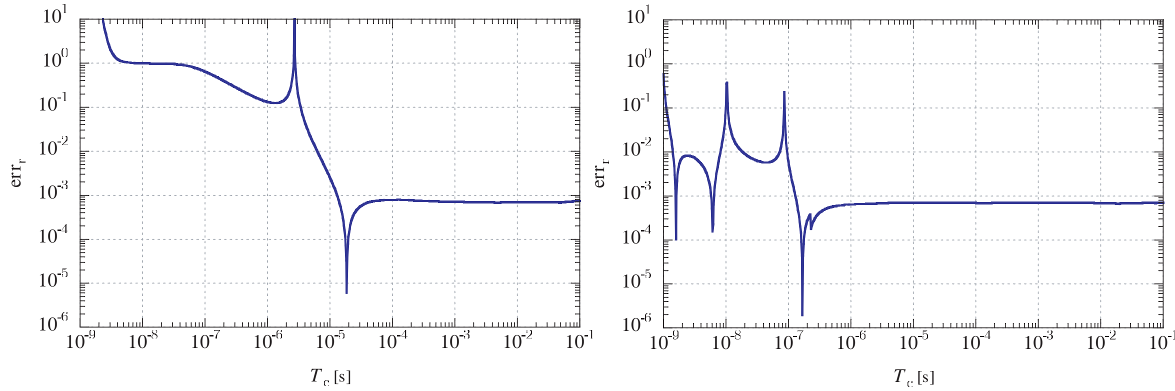

(a) (b)

Figure 3. Relative error $\mathrm{err_r}$ at the observation time $t = 2T_\mathrm{c}$ as a function of the characteristic time T_c for the same structure as in Fig. 2 with (a) $h = 30\,\mu\mathrm{m}$ and (b) $h = 1\,\mu\mathrm{m}$.

In Fig. 3(a), the relative error $\mathrm{err_r}$ is reported as a function of the characteristic time T_c. The relative error is defined as

$$\mathrm{err_r}(t) = \frac{\left| e_y^{\mathrm{ex}}(t) - e_y^{\mathrm{app}}(t) \right|}{e_y^{\mathrm{ex}}(t)} \tag{37}$$

where e_y^{ex} and e_y^{app} represent the electric field calculated through (1)–(4) and (15)–(18), respectively, and is calculated at an observation time $t = 2T_\mathrm{c}$. By reducing the screen thickness to $h = 1\,\mu\mathrm{m}$, from (36) it follows that the semi-analytical formulation is certainly accurate from $T_\mathrm{c} > 130\,\mathrm{ns}$. This is confirmed in Fig. 3(b) where the relative error $\mathrm{err_r}$ is reported as a function of the characteristic time T_c for this new structure.

Therefore, in general, the accuracy of the semi-analytical formulation depends on the combination of the metal conductivity σ, the screen thickness h, and the characteristic time of the source T_c.

7. NUMERICAL RESULTS

We consider a thin conductive screen constituted by a conductive painting over a foam support. The considered film is a conductive carbon painting available in commerce having a thickness $h = 1$ mil ($25\,\mu\mathrm{m}$) and a surface resistance $R_\mathrm{s} = 47\,\Omega/\mathrm{sq}$ (as taken from available datasheet) which corresponds to a conductivity $\sigma = 8.51 \cdot 10^2\,\mathrm{S/m}$. The line source is located at $(x_0, z_0) = (0, 0.1)\,\mathrm{m}$ and the observation point for SE evaluations is at $(x, z) = (0, -0.1)\,\mathrm{m}$. Both a PEP and an MP sources are considered with $T_\mathrm{c} = 20\,\mathrm{ns}$ and the relevant incident electric and magnetic field at the observation point are reported as a function of t/T_c in Figs. 4(a) and 4(b), respectively.

The relevant transmitted field are reported in Figs. 5(a) and 5(b), respectively, where also the perfect agreement between the exact numerical and the approximate semianalytical formulations is shown. Based on the results of Figs. 4 and 5 it results $\mathrm{SE}_{\mathrm{PR}}^{\mathrm{E}} = 7.83\,\mathrm{dB}$ and $\mathrm{SE}_{\mathrm{PR}}^{\mathrm{H}} = 3.2\,\mathrm{dB}$ for the transient PEP source and $\mathrm{SE}_{\mathrm{PR}}^{\mathrm{E}} = 9.37\,\mathrm{dB}$ and $\mathrm{SE}_{\mathrm{PR}}^{\mathrm{H}} = 4.4\,\mathrm{dB}$ for the transient MP source. For coinciseness, the relevant plots for the time-derivative of the fields are not reported, but it is easily to show that it results $\mathrm{SE}_{\mathrm{DR}}^{\mathrm{E}} = 9.36\,\mathrm{dB}$ and $\mathrm{SE}_{\mathrm{DR}}^{\mathrm{H}} = 4.33\,\mathrm{dB}$ for the transient PEP source and $\mathrm{SE}_{\mathrm{DR}}^{\mathrm{E}} = 9.58\,\mathrm{dB}$ and $\mathrm{SE}_{\mathrm{DR}}^{\mathrm{H}} = 6.02\,\mathrm{dB}$ for the transient MP source.

For a fair comparison, the relevant electric and magnetic FD SE for a *time-harmonic* electric line source are reported in Fig. 6 as functions of the radian frequency ω. It is interesting to note that at the radian frequency $\omega_\mathrm{c} = 2\pi/T_\mathrm{c}$, the FD SE values ($\mathrm{SE_E} = 9.1\,\mathrm{dB}$ and $\mathrm{SE_H} = 5.5$ dB) are close to the corresponding TD SE values.

Finally, we consider a more realistic transient source, i.e., an indirect electrostatic discharge (ESD). The field radiated by the indirect ESD has been simulated as that due to a known current flowing through

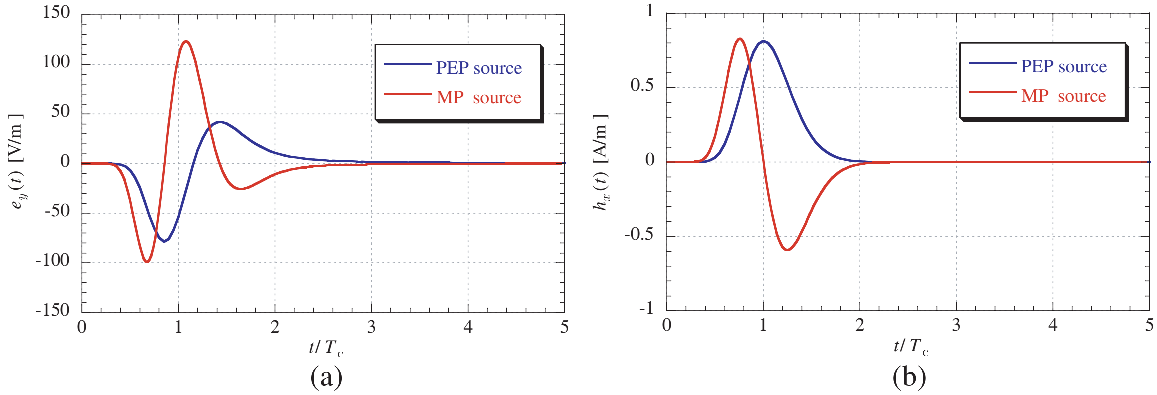

Figure 4. Time-domain incident fields corresponding to a PEP and an MP transient source with $I_0 = 1$ A, $T_c = 20$ ns, and $n = 16$. Other parameters: $\Delta x = 0$, $\Delta z = 20$ cm.

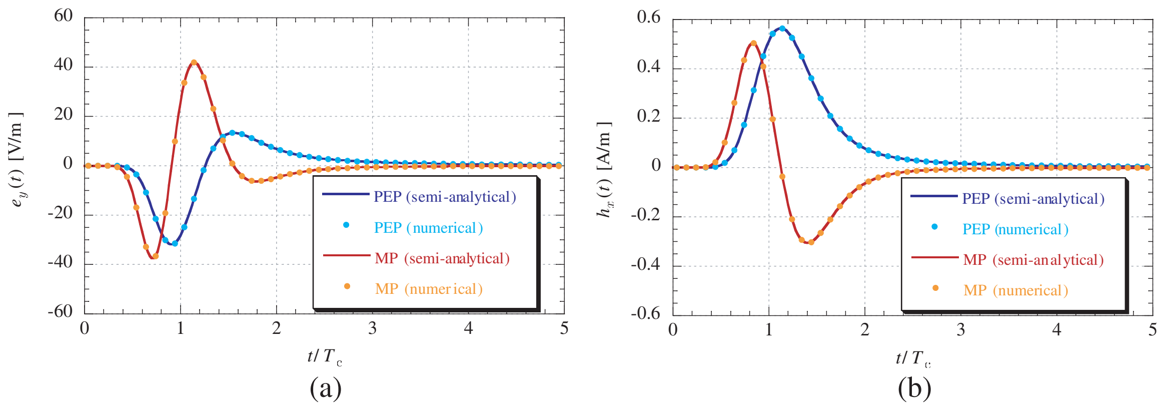

Figure 5. Time-domain transmitted fields corresponding to a PEP and an MP transient source as in Fig. 4 for a conductive screen with parameters $h = 25$ µm and $\sigma = 8.51 \cdot 10^2$ S/m.

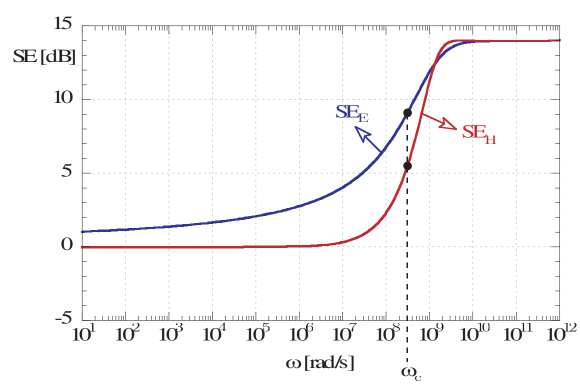

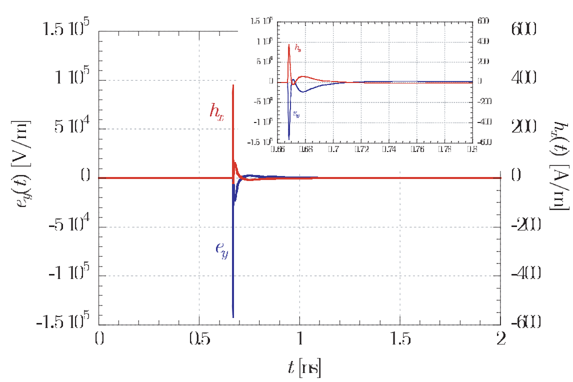

Figure 6. Electric and magnetic frequency-domain shielding effectiveness as functions of the radian frequency ω for a time-harmonic electric line source.

Figure 7. Time-domain incident fields corresponding to the ESD line source with parameters as in Table 1. Other parameters: same as in Fig. 4. In the inset the details of the time interval between 0.66 ns and 0.8 ns are shown.

a conductive path [18, 19] and its waveform is assumed to be given by the following expression [20]:

$$i(t) = I_0(1 - \exp[-t/\tau_1])^{n_0} \exp[-t/\tau_2] + I_1(1 - \exp[-t/\tau_3])^{n_1} \exp[-t/\tau_4] \\ + I_2(1 - \exp[-t/\tau_5])^{n_2} \exp[-t/\tau_6], \quad (38)$$

Table 1. Parameters of ESD waveform.

Amplitude [A]	*Time constant* [ns]	*Time constant* [ns]	*Exponent*
$I_0 = 53.5$	$\tau_1 = 0.606$	$\tau_2 = 1.759$	$n_0 = 5$
$I_1 = 27.9$	$\tau_3 = 5.0$	$\tau_4 = 14.220$	$n_1 = 5$
$I_2 = 19.2$	$\tau_5 = 18.170$	$\tau_6 = 38.260$	$n_2 = 3$

where the values of the parameters I_k and τ_k are reported in Table 1, along with the exponents n_k.

The corresponding TD incident fields for the same geometry previously considered are reported in Fig. 7.

The FD electric fields calculated with the exact and the approximate SD Green's functions are reported in Fig. 8 showing a perfect agreement.

The relevant transmitted TD electric and magnetic fields are finally reported in Fig. 9 in the time range where they have non-negligible values. Interestingly, based on these results one obtains $\mathrm{SE}_{\mathrm{PR}}^{\mathrm{E}} = \mathrm{SE}_{\mathrm{PR}}^{\mathrm{H}} = 13.99\,\mathrm{dB}$, while $\mathrm{SE}_{\mathrm{DR}}^{\mathrm{E}} = 13.98\,\mathrm{dB}$ and $\mathrm{SE}_{\mathrm{DR}}^{\mathrm{H}} = 14.02\,\mathrm{dB}$, which are significantly larger values with respect to those obtained with PEP and MP sources.

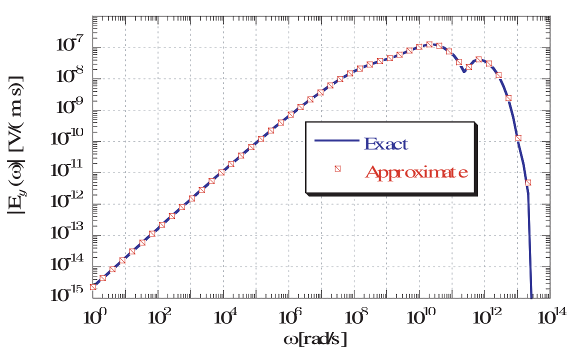

Figure 8. Frequency-domain electric fields calculated through the exact and approximate SD Green's functions as functions of the radian frequency ω for the ESD line source with parameters as in Table 1 and for a screen with parameters as in Fig. 5.

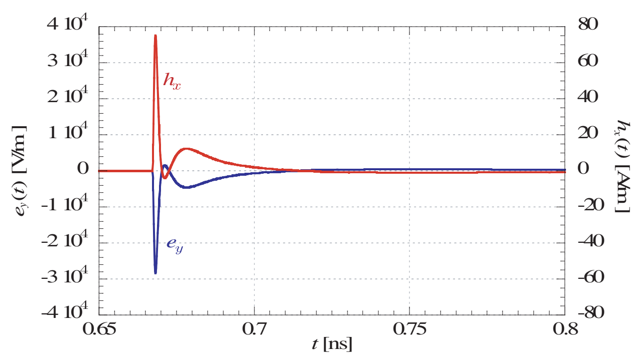

Figure 9. Time-domain transmitted fields corresponding to an ESD electric fline source with incident fields as in Fig. 7. Screen parameters are the same as in Fig. 5.

8. CONCLUSIONS

The shielding performance of planar conductive screens against transient line sources has been studied in detail by means of an approximate semi-analytical formulation based on a Cagniard-De Hoop approach and an exact numerical double inverse-Fourier transform analysis. The limits of validity of the semi-analytical results, which have the great advantage to allow for the expression of all the field components as a simple time convolution, have been critically discussed. New time-domain shielding effectiveness parameters recently proposed in the literature have been considered for different transient sources, showing how the shielding performance can strongly depend on the transient behavior of the electromagnetic source. The analysis of time-domain shielding effectiveness of conductive screen with a frequency-dependent conductivity (such as graphene sheets) and in the presence of dipole sources is currently in progress.

REFERENCES

1. Lee, K., *EMP Interaction: Principles, Techniques, and Reference Data: A Handbook of Technology from the EMP Interaction Notes*, Taylor & Francis/Hemisphere, 1986.
2. Araneo, R. and S. Celozzi, "Toward a definition of the shielding effectiveness in the time-domain," *Proc. IEEE Electromagn. Compat. Symp.*, 113–117, Aug. 5–9, 2013.
3. Celozzi, S. and R. Araneo, "TD-Shielding effectiveness of enclosures in presence of ESD," *Proc. EMC Europe Symp.*, 541–544, Sep. 2–6, 2013.
4. Celozzi, S., R. Araneo, and G. Lovat, *Electromagnetic Shielding*, Wiley-IEEE, Hoboken, 2008.
5. Lovat, G., P. Burghignoli, and S. Celozzi, "Shielding properties of a wire-medium screen," *IEEE Trans. Electromagn. Compat.*, Vol. 50, No. 1, 80–88, Feb. 2008.
6. Lovat, G., "Near-field shielding effectiveness of 1-D periodic planar screens with 2-D near-field sources," *IEEE Trans. Electromagn. Compat.*, Vol. 51, No. 3, 708–719, Aug. 2009.
7. Araneo, R., G. Lovat, and S. Celozzi, "Shielding effectiveness of periodic screens against finite high-impedance near-field sources," *IEEE Trans. Electromagn. Compat.*, Vol. 53, No. 3, 706–716, Aug. 2011.
8. Wang, Y.-L., W. Ren, and K. Li, "Exact transient field of a horizontal electric dipole excited by a gaussian pulse on the surface of one-dimensionally anisotropic medium," *Progress In Electromagnetics Research B*, Vol. 8, 307–318, 2008.
9. Popov, A. V. and V. V. Kopeikin, "Electromagnetic pulse propagation over nonuniform earth surface: numerical simulation," *Progress In Electromagnetics Research B*, Vol. 6, 37–64, 2008.
10. De Hoop, A. T. and L. Combee, "Transient diffusive electromagnetic fields in layered media — An analysis based on the Cagniard method," *PIERS Proceedings*, 520, Boston, MA, USA, Jul. 25–26, 1989.
11. Chew, W. C., *Waves and Fields in Inhomogenous Media*, IEEE Press, Piscataway, NJ, 1999.
12. De Hoop, A. T., L. L. Meng, and L. J. Jiang, "Pulsed line source response of a thin sheet with high-contrast dielectric and conductive properties — A time domain analysis," *IEEE Trans. Antennas Propag.*, Vol. 61, No. 11, 5649–5657, Nov. 2013.
13. Michalski, K. A. and J. R. Mosig, "Multilayered media Green's functions in integral equation formulations," *IEEE Trans. Antennas Propag.*, Vol. 45, No. 3, 508–519, Mar. 1997.
14. Mosig, J., "The weighted averages algorithm revisited," *IEEE Trans. Antennas Propag.*, Vol. 60, No. 4, 2011–2018, Apr. 2012.
15. De Hoop, A. T. and M. L. Oristaglio, "Application of the modified CAgniard technique to transient electromagnetic diffusion problems," *Geophysical Journal*, Vol. 94, 387–397, 1988.
16. De Hoop, A., "A modification of Cagniard's method for solving seismic pulse problems," *Applied Scientific Research, Section B*, Vol. 8, No. 1, 349–356, 1960.
17. Celozzi, S., "New figures of merit for the characterization of the performance of shielding enclosures," *IEEE Trans. Electromagn. Compat.*, Vol. 46, No. 1, 142–142, Feb. 2004.
18. Muchaidze, G., J. Koo, Q. Cai, T. Li, L. Han, A. Martwick, K. Wang, J. Min, J. L. Drewniak, and D. Pommerenke, "Susceptibility scanning as a failure analysis tool for system-level electrostatic discharge (ESD) problems," *IEEE Trans. Electromagn. Compat.*, Vol. 50, No. 2, 268–276, 2008.
19. Cerri, G., R. De Leo, R. De Rentiis, and V. M. Primiani, "ESD field penetration through slots into shielded enclosures: A time domain approach," *IEEE Trans. Electromagn. Compat.*, Vol. 39, No. 4, 377–386, 1997.
20. Yuan, Z., T. Li, J. He, and R. Zeng, "New mathematical descriptions of ESD current waveform based on the polynomial of pulse function," *IEEE Trans. Electromagn. Compat.*, Vol. 48, No. 3, 589–591, 2006.